Springer

Journal of
Mechanical
Science and
Technology

Journal of Mechanical Science and Technology 23 (2009) 2964~2972

www.springerlink.com/content/1738-494x
DOI 10.1007/s12206-009-0814-5

# Crack identification in a rotor with an open crack †

Guang Ming Dong* and Jin Chen

*The State Key Laboratory of Mechanical System & Vibration, Shanghai Jiao Tong University, Shanghai, 200240, P. R. China*

(Manuscript Received March 26, 2008; Revised June 19, 2009; Accepted July 26, 2009)

**Abstract**

A finite element (FE) model, which is based on a transfer matrix analysis and local flexibility theorem, is introduced for crack identification of a static (non-rotating) rotor with an open crack. Through numerical simulation, the effects of crack location and crack depth on the mode shapes and the changes in the eigenfrequencies of the cracked rotor are investigated. A crack identification algorithm that makes use of the translations of the first mode at two symmetric points and the contour diagram of crack location versus crack depth for the first two given normalized eigenfrequencies is proposed to estimate the crack location and depth in the rotor. Two illustrative examples are demonstrated and compared for availability and validity of the proposed algorithm.

***Keywords***: Cracked rotor; Eigenfrequency; Finite element analysis; Local flexibility; Mode shape; Transfer matrix analysis

## 1. Introduction

One form of damage that can lead to catastrophic failure if undetected is fatigue cracking of the shaft. Thus, the early detection of cracked rotor in engineering practices is significantly important for the reliability and durability of large rotating machinery. In effect, fault diagnosis and condition monitoring of cracked rotor has been given more and more attention in recent years [1-6]. For the time being, research on cracked rotor still remains at the theoretical stage, and most of the previous research studies only involve crack detection in a rotor and not the crack location and depth.

A static (non-rotating) rotor with an open crack can be considered simply as a supported beam. As a consequence, research in relation to non-rotating structures such as beams and columns is useful for locating and estimating the severity of cracks in a rotor [7-13]. Adams found that a state of damage could be detected by the reduction in stiffness and an increase in damping, whether the damage was localized (as in a crack) or as many microcracks distributed throughout the bulk of the specimen [14]. Using the receptance technique and the Taylor series expansion, Cawley and Adams showed that the ratio of the frequency changes in the two modes is only a function of the damaged location, respectively [15]. In Ref. [16], the effect of a crack on the deformation of a beam has been considered similar to that of an elastic hinge, and the local flexibility due to the crack is computed with fracture mechanics methods and measured experimentally. Rizos estimated the crack location and depth with satisfactory accuracy from the measured amplitudes at two points of the structure vibrating at one of its natural modes, the respective vibration frequency, and identified an analytical solution of the dynamic response [17]. For a rotor removed from service, Inagaki used natural vibration and the static deflection analysis to find the crack size and location [18]. Meanwhile, Rajab presented analytical expressions and derived the curves relating the

† This paper was recommended for publication in revised form by Associate Editor Eung-Soo Shin

*Corresponding author. Tel.: +86 21 3420 6831, Fax.: 86 21 3420 6006
E-mail address: gmdong@sjtu.edu.cn

crack depth and location in a cracked Timoshenko shaft to the changes in the natural frequencies. Its numerical simulation showed that knowledge of the changes in the first three natural frequencies relative to the uncracked shaft is sufficient in estimating the crack location and depth in the shaft [19]. By perturbation theory and transfer matrix analysis, Gudmundson calculated the variation of eigenfrequencies due to a crack on a cantilever beam [20, 21]. Following Gudmundson, Gounaris proposed a finite element model using the transfer matrix method and local flexibility theorem. To consider the discontinuity deformation due to the crack on the beam, he adopted two different shape functions for the two segments separated by the crack [22]. Based on the research of Gudmundson and Gounaris, Nikolakopoulos presented the dependency of the structural eigenfrequencies on crack depth and location in contour graph form. To identify the location and depth of a crack, the intersection points of the superposed contours that correspond to the measured eigenfrequency variations and caused by the presence of the crack should be determined [23]. With the model from Nikolakopoulos, Suh presented a detection method that uses the hybrid neuro-genetic technique to identify the location and depth of a crack on a structure [24]. Hu and Liang proposed a two-step procedure to identify cracks in beam structures. They used the effective stress concept coupled with Hamilton's principle to derive a formulation relating the changes in the natural frequencies to the changes in member stiffness. While using the formulation, the elements containing the cracks could be identified. The spring damage model was used to quantify the location and depth of the crack in each damaged element [25].

In this paper, a finite element (FE) model is introduced for crack identification in a static (non-rotating) rotor with an open crack. The effects of the location and depth of the crack on the mode shapes and the changes in the eigenfrequencies of the cracked rotor are investigated. A crack identification algorithm is proposed to estimate the crack location and depth in the rotor, and two illustrative examples are demonstrated and compared for availability and validity of the proposed algorithm.

## 2. Finite element model

In Ref. [21-23], transfer matrix analysis is introduced for the derivation of the stiffness matrix of the cracked element, and the FE model for the cantilever beam is presented. The present study uses an FE model simplified from the model by Ref. [21-23] to investigate the flexural vibration characteristics of a cracked rotor.

A non-rotating rotor with a single open crack with depth $a_d$ and location $Z_1$ can be discretized into $n$ beam elements or subsystems. The schematic diagram is shown in Fig. 1, where each element has one translational and one rotational degree of freedom (DOF) for flexural vibration at each node. A crack on a beam element results in local flexibility due to the strain energy concentration near the crack tip under the load. According to the principle of Saint-Venant, the stress field is affected only in the region adjacent to the crack; the element stiffness matrix, except for the cracked element, may be regarded as unchanged under a certain limitation of element size [8]. For the uncracked beam element shown in Fig. 2, the corresponding stiffness and consistent mass matrices are given as follows:

$$\mathbf{K}_e = \frac{EI}{l^3}\begin{bmatrix} 12 & 6l & -12 & 6l \\ 6l & 4l^2 & -6l & 2l^2 \\ -12 & -6l & 12 & -6l \\ 6l & 2l^2 & -6l & 4l^2 \end{bmatrix} \tag{1}$$

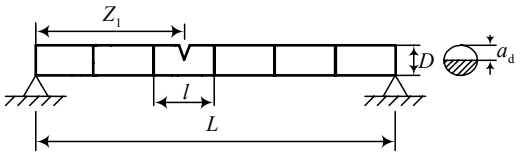


Fig. 1. Diagram of a rotor with a single open crack.

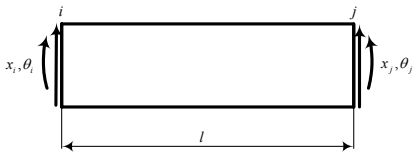


Fig. 2. Uncracked beam element.

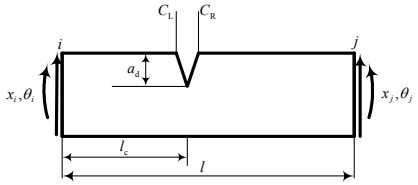


Fig. 3. Cracked beam element.

$$\mathbf{M}_{\mathrm{e}}=\frac{\rho Al}{420}\begin{bmatrix}156 & 22l^2 & 54 & -13l\\ 22l & 4l^2 & 13l & -3l^2\\ 54 & 13l & 156 & -22l\\ -13l & -3l^2 & -22l & 4l^2\end{bmatrix} \tag{2}$$

A cracked beam finite element with a crack depth $a_{\mathrm{d}}$ at location $l_{\mathrm{c}}$ from its left endpoint is depicted in Fig. 3. Suppose that the crack only affects the stiffness, and the element mass matrix is invariant. Due to the discontinuity of deformation in the cracked element, it is very difficult to determine an appropriate shape function to express approximately the kinetic energy and elastic potential energy. To derive the stiffness matrix of the cracked element, the transfer matrix analysis that transfers the state variables (generalized displacements and forces) from one node to the other node is adopted (21)-(23), (26). The state vectors at positions $i$, $j$, $C_{\mathrm{L}}$, and $C_{\mathrm{R}}$ are as follows:

$$\mathbf{V}_i=\{x_i,\theta_i,F_i,M_i\}^T \tag{3a}$$
$$\mathbf{V}_j=\{x_j,\theta_j,F_j,M_j\}^T \tag{3b}$$
$$\mathbf{V}_{\mathrm{L}}=\{x_{\mathrm{L}},\theta_{\mathrm{L}},F_{\mathrm{L}},M_{\mathrm{L}}\}^T \tag{3c}$$
$$\mathbf{V}_{\mathrm{R}}=\{x_{\mathrm{R}},\theta_{\mathrm{R}},F_{\mathrm{R}},M_{\mathrm{R}}\}^T \tag{3d}$$

From the Euler-Bernoulli theory, the state vectors can be related as follows:

$$\mathbf{V}_{\mathrm{L}}=\mathbf{T}_{\mathrm{l}}\mathbf{V}_i \tag{4a}$$
$$\mathbf{V}_{\mathrm{R}}=\mathbf{T}_{\mathrm{c}}\mathbf{V}_{\mathrm{L}} \tag{4b}$$
$$\mathbf{V}_j=\mathbf{T}_2\mathbf{V}_{\mathrm{R}}, \tag{4c}$$

where

$$\mathbf{T}_{\mathrm{l}}=\begin{bmatrix}1 & l_{\mathrm{c}} & \dfrac{l_{\mathrm{c}}^3}{6EI} & -\dfrac{l_{\mathrm{c}}^2}{2EI}\\ 0 & 1 & \dfrac{l_{\mathrm{c}}^2}{2EI} & -\dfrac{l_{\mathrm{c}}}{EI}\\ 0 & 0 & -1 & 0\\ 0 & 0 & l_{\mathrm{c}} & -1\end{bmatrix} \tag{5a}$$

$$\mathbf{T}_2=\begin{bmatrix}1 & l-l_{\mathrm{c}} & \dfrac{(l-l_{\mathrm{c}})^3}{6EI} & -\dfrac{(l-l_{\mathrm{c}})^2}{2EI}\\ 0 & 1 & \dfrac{(l-l_{\mathrm{c}})^2}{2EI} & -\dfrac{l-l_{\mathrm{c}}}{EI}\\ 0 & 0 & -1 & 0\\ 0 & 0 & l-l_{\mathrm{c}} & -1\end{bmatrix} \tag{5b}$$

Due to the crack, the point transfer matrix $\mathbf{T}_{\mathrm{c}}$, which relates the state vectors on the left and right sides of the crack, is

$$\mathbf{T}_{\mathrm{c}}=\begin{bmatrix}1 & 0 & c_{11} & 0\\ 0 & 1 & 0 & c_{22}\\ 0 & 0 & -1 & 0\\ 0 & 0 & 0 & -1\end{bmatrix} \tag{5c}$$

With regard to the cross section of a cracked rotor shown in Fig. 4, the local flexibility $c_{11}$, $c_{22}$ can be calculated as

$$\bar{c}_{11}=\int_{-b/R}^{+b/R}\mathrm{d}\frac{\eta}{R}\int\frac{2}{\pi}\frac{z}{R}F_{II}^2(\frac{z}{h})\mathrm{d}\frac{z}{R} \tag{6a}$$

$$\bar{c}_{22}=\int_{-b/R}^{+b/R}\mathrm{d}\frac{\eta}{R}\int\frac{32}{\pi^2}[1-(\frac{z}{R})^2]\pi\frac{z}{R}F_2^2(\frac{z}{h})\mathrm{d}\frac{z}{R} \tag{6b}$$

where

$$b=\sqrt{R^2-(R-a_{\mathrm{d}})^2} \tag{7a}$$

$$F_{II}(\frac{z}{h})=\frac{1.122-0.561\dfrac{z}{h}+0.085(\dfrac{z}{h})^2+0.18(\dfrac{z}{h})^3}{\sqrt{1-\dfrac{z}{h}}} \tag{7b}$$

$$h=2\sqrt{R^2-\eta^2} \tag{7c}$$

$$F_2(\frac{z}{h})=\sqrt{\frac{2h}{\pi z}\tan\frac{\pi z}{2h}}\cdot\frac{0.923+0.199(1-\sin\dfrac{\pi z}{2h})^4}{\cos\dfrac{\pi z}{2h}} \tag{7d}$$

Calculated by Simpson integration, the variations of the dimensionless flexibility with the relative crack depth $a_{\mathrm{d}}/R$ are shown in Fig. 5.

From Eqs. 4(a-c), the following relation is obtained:

$$\mathbf{V}_j=\mathbf{T}_{\mathrm{e}}^{\mathrm{c}}\mathbf{V}_i. \tag{8}$$

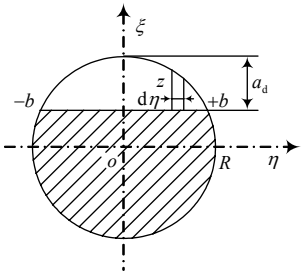


Fig. 4. Cross section of a cracked rotor.

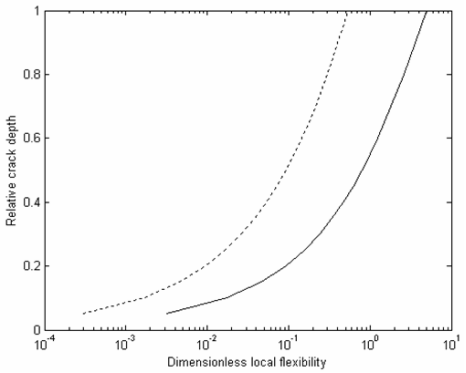


Fig. 5. Dimensionless local flexibility due to the crack.(··· $\bar{c}_{11}$, – $\bar{c}_{22}$)

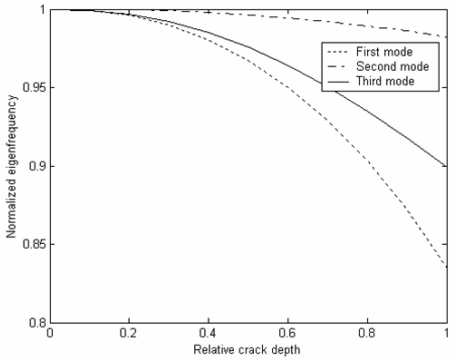


Fig. 6. Variations of the normalized eigenfrequencies with relative crack depth for a rotor with a certain slenderness ratio and crack location.

The transfer matrix $\mathbf{T}_e^c$ of the cracked element is written in the following form:

$$\mathbf{T}_e^c = \mathbf{T}_2\mathbf{T}_c\mathbf{T}_1 = \begin{bmatrix} \mathbf{T}_{11} & \mathbf{T}_{12} \\ \mathbf{T}_{21} & \mathbf{T}_{22} \end{bmatrix}, \tag{9}$$

and the stiffness matrix of the cracked element can be readily computed [23], [24] as

$$\mathbf{K}_e^c = \begin{bmatrix} -\mathbf{T}_{12}^{-1}\mathbf{T}_{11} & \mathbf{T}_{12}^{-1} \\ \mathbf{T}_{21} - \mathbf{T}_{22}\mathbf{T}_{12}^{-1}\mathbf{T}_{11} & \mathbf{T}_{22}\mathbf{T}_{12}^{-1} \end{bmatrix}. \tag{10}$$

Assembling the element stiffness and consistent mass matrices to obtain the global stiffness and mass matrices, the model of the cracked rotor in bending is set up in the following form:

$$(-\omega^2\mathbf{M} + \mathbf{K})\mathbf{x} = \{\mathbf{0}\}. \tag{11}$$

Based on the above equation, the eigenvalue analysis is carried out and used to investigate the vibration characteristics of a rotor with a single open crack.

## 3. Vibration analysis

In the simulation, the rotor geometries and material properties are given as follows: $L = 3$ m, $\nu = 0.3$, $E = 2.07\times10^{11}$ N/m$^2$, and $\rho = 7.7\times10^3$ kg/m$^3$.

### *3.1 Effects of the relative crack depth*

For a rotor with a slenderness ratio $L/D = 8$ and crack location $Z_1/L = 0.45$, a parametric study of the effect of the crack depth on the vibration characteristics of the rotor is carried out by varying the relative crack depth $\bar{a}_d = a_d/R$. The cracked rotor is discretized into 10 beam elements. The variations of the first three normalized eigenfrequencies $\omega_{ci}/\omega_{ni}$ ($i = 1,2,3$) with the relative crack depth are shown in Fig. 6. For a given crack location, it can be seen from Fig. 6 that for a given crack location, the changes in eigenfrequencies of the cracked rotor monotonically increase with the increment of the crack depth, such that if the crack location is known in advance, the crack depth can be read out from the changes in eigenfrequencies. It can also be seen from Fig. 6 that the change in the first eigenfrequency with a crack present is significant because the crack is close to the antinodal point of the first mode. In contrast, the change in the second eigenfrequency is quite small because the crack is near the nodal point of that mode. In addition, a large drop in the eigenfrequencies results from the increment of crack depth for a given crack location in the rotor. Thus, it can be concluded from Fig.6 that if the crack location is known in advance, the crack depth can be read out from the changes in eigenfrequencies.

### *3.2 Effects of the crack location*

For a cracked rotor with a slenderness ratio $L/D$=8 and certain relative crack depths $\bar{a}_d = 0.2, 0.4, 0.6, 0.8, 1.0$, the variations of eigenfrequencies with different crack locations $Z_1/L$ are shown in Fig. 7. It is clear that the changes in the first two normalized eigenfrequencies $\omega_{ci}/\omega_{ni}$ ($i = 1,2$) show a symmetric property because the symmetry of the rotor is considered. It can be concluded from Fig. 7 that the changes in normalized eigenfrequencies depend on how close the crack is to that the mode of shape node, that is, the

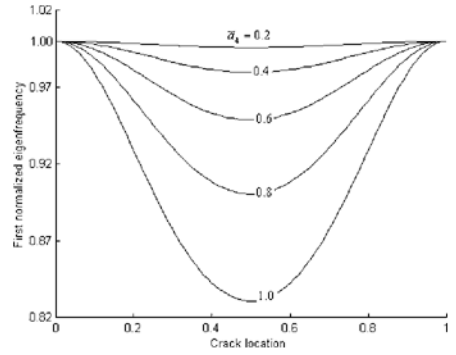


(a) Variation of the first normalized eigenfrequency

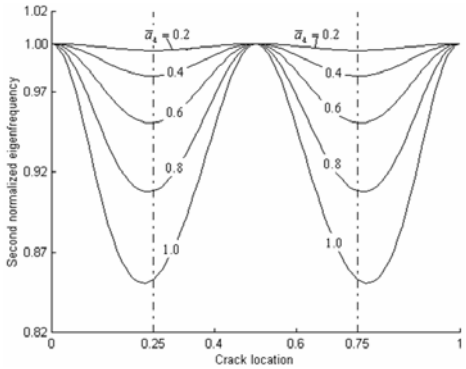


(b) Variation of the second normalized eigenfrequency

Fig. 7. Variations of normalized eigenfrequencies with crack location as a relative crack depth is invariable.

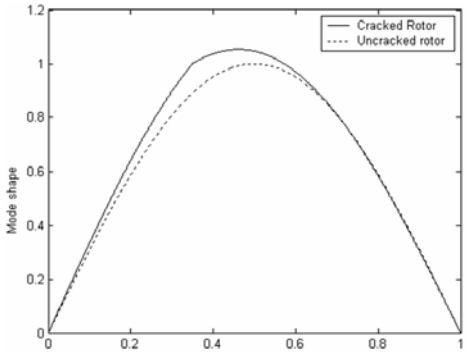


(a) First mode

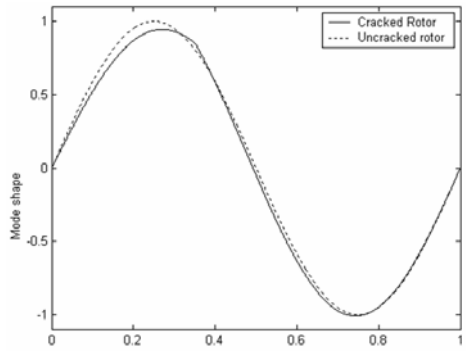


(b) Second mode

Fig. 8. Mode shapes of a rotor with a certain slenderness ratio, crack location, and relative crack depth.

reduction in the eigenfrequency of a mode is larger if the crack is near the antinodal point of that mode shape.

As the relative crack depth and variations of eigenfrequencies are known, two possible crack locations are obtained. Combining the previous discussion on the effects of relative crack depth, a contour diagram of crack location versus crack depth for the first two normalized eigenfrequencies is used to obtain two possible cracks.

### *3.3 Comparison of the mode shapes between the cracked and uncracked rotor*

The corresponding mode shapes for the first two eigenfrequencies of the rotor with slenderness ratio $L/D=8$, crack location $Z_1/L=0.45$, and relative crack depth $\bar{a}_{\mathrm{d}}=0.6$ are shown in Fig. 8, wherein the cracked rotor is discretized into 100 beam elements for better resolution. In Fig. 8, the changes in the first mode shapes are more obvious on the left side of the rotor, which show that the first mode shape is helpful in selecting the true crack location from the two possible cracks.

## 4. Crack identification

Based on the above analysis, a crack identification algorithm is proposed, in which the contour diagram of the crack location versus crack depth for the first two normalized eigenfrequencies is calculated to estimate two symmetric candidates for crack location and depth. The deflections of the first mode are then used to erase the symmetric property and determine the actual crack location. That is, if the deflection of the point on the left side of the rotor is larger than that of the point on the right side, the crack is located on the left side of the rotor, otherwise on the right side. The flow chart of the algorithm is presented in Fig. 9.

The first crack identification problem is stated as follows. The slenderness ratio of a cracked rotor is $L/D=8$, and the first two normalized eigenfrequencies are $\omega_{\mathrm{c1}}/\omega_{\mathrm{n1}}=0.9980$ and $\omega_{\mathrm{c2}}/\omega_{\mathrm{n2}}=0.9959$. The contour diagram of the crack location versus crack depth for the given normalized eigenfrequencies is shown in Fig. 10. In Fig. 10, the read out

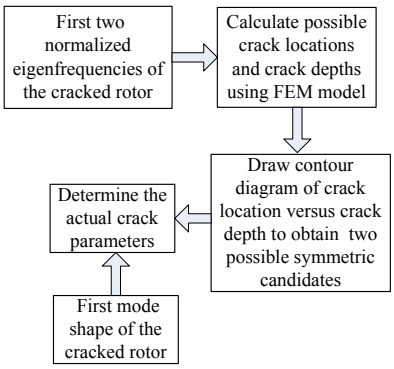


Fig. 9. Flow chart of the crack identification algorithm.

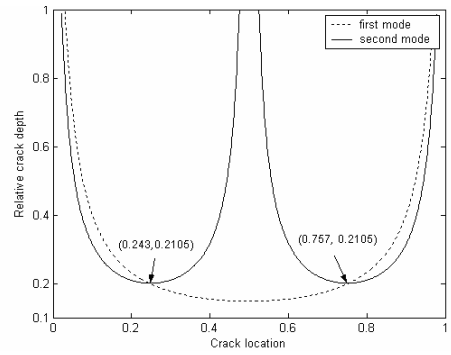


Fig. 10. Contour diagram of the crack location versus crack depth for first two normalized eigenfrequencies $\omega_{c1}/\omega_{n1} = 0.9980$, $\omega_{c2}/\omega_{n2} = 0.9959$ of the cracked rotor.

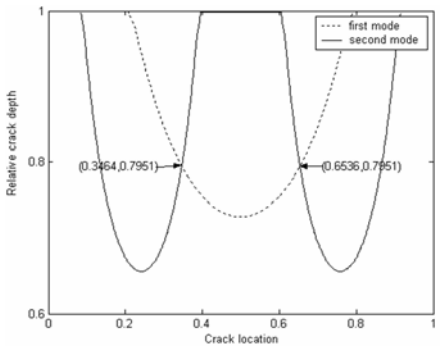


Fig. 11. Contour diagram of the crack location versus crack depth for first two normalized eigenfrequencies $\omega_{c1}/\omega_{n1} = 0.9181$, $\omega_{c2}/\omega_{n2} = 0.9411$ of the cracked rotor.

shows that the two possible crack locations are $Z_1/L = 0.243$ and $Z_1/L = 0.757$, and the relative crack depth is $\bar{a}_d = 0.2105$. The deflections of the two symmetric points on the left and right sides are 0.72 and 0.7, respectively. As the deflection of the point on the left side of the rotor is larger than that of the point on the right side, the crack is located on the left side of the rotor. The crack location $Z_1/L = 0.243$ and the relative crack depth $\bar{a}_d = 0.2105$ are the final predicted results.

Table 1. Comparison between the predicted and actual results of the first example.

| | Predicted results | Actual results | Errors |
|---|---|---|---|
| $Z_1/L$ | 0.243 | 0.25 | 2.8% |
| $\bar{a}_d$ | 0.2105 | 0.2 | 5.25% |

Table 2. Comparison between the predicted and actual results of the second example.

| | Predicted results | Actual results | Errors |
|---|---|---|---|
| $Z_1/L$ | 0.3464 | 0.35 | 1% |
| $\bar{a}_d$ | 0.7951 | 0.8 | 0.6% |

The second crack identification problem is stated as follows. The slenderness ratio of a cracked rotor is $L/D = 8$, and the first two normalized eigenfrequencies are $\omega_{c1}/\omega_{n1} = 0.9181$ and $\omega_{c2}/\omega_{n2} = 0.9411$. The deflections of the two symmetric points on the left and right sides are 1.0005 and 0.9002, respectively. As the deflection of the point on the left side of the rotor is larger than that of the point on the right side, the crack is located on the left side of the rotor. The contour diagram of the crack location versus crack depth for the given normalized eigenfrequencies is shown in Fig. 11. According to this figure, the two possible crack locations are $Z_1/L = 0.3464$ and $Z_1/L = 0.6536$, and the relative crack depth is $\bar{a}_d = 0.7951$. As the crack is located on the left side of the rotor, the crack location $Z_1/L = 0.3464$ and the relative crack depth $\bar{a}_d = 0.7951$ are the final predicted results.

The predicted crack depth and location are compared with the actual results in Tables 1 and 2. It can be seen that the error is very small, illustrating the validity of the proposed crack identification algorithm. Compared with the results in Ref. [27], in which a continuous model of cracked rotor is presented, the prediction error is slightly larger for the FE model of this paper. However, the FE model has more flexibility for engineering requirements.

## 5. Conclusion

An FE model is introduced for crack identification of a static (non-rotating) rotor with an open crack. The stiffness matrix of the cracked element is ob-

tained using transfer matrix analysis and local flexibility theorem.

The changes in eigenfrequencies monotonically increase with the increment of the crack depth for a given crack location in a cracked rotor. Because of the symmetry of the rotor, the changes in eigenfrequencies with different crack locations show a symmetric property, and their changes depend on how close the crack is to one of the mode shape nodes. If the first two eigenfrequencies are known in advance, two possible cracks can be predicted at the symmetric locations on the rotor, but the first mode shape can be used to select the true crack location from the two possible cracks.

A crack identification algorithm that makes use of the translations of the first mode at two symmetric points and contour diagram of crack location versus crack depth for first two given normalized eigenfrequencies is proposed to estimate the crack location and depth in the rotor. Two illustrative examples are demonstrated and compared for the availability and validity of the proposed algorithm.

## Acknowledgment

We gratefully acknowledge the support from the National Natural Science Foundation (Approved Grant: 50875162) and the China Postdoctoral Science Foundation funded project (Approved Grant: 20070-420655).

## Nomenclature

$a_d$ : Crack depth
$\bar{a}_d$ : Relative crack depth
$Z_1$ : Crack location of the rotor
$A$ : Cross-sectional area
$L$ : Length of the rotor
$R$ : Radius of the rotor
$D$ : Diameter of the rotor
$E$ : Young's modulus
$v$ : Poisson ratio
$\rho$ : Material density
$I$ : Moment of inertia
$l$ : Length of the element
$l_c$ : Crack location from the left endpoint on an element
$c_{11}$, $c_{22}$ : Local flexibility
$\bar{c}_{11}$, $\bar{c}_{22}$ : Dimensionless flexibility
$\mathbf{K}$ : Global stiffness matrix
$\mathbf{K}_e$ : Stiffness matrix of uncracked element
$\mathbf{K}_e^c$ : Stiffness matrix of cracked element
$\mathbf{M}$ : Global mass matrix
$\mathbf{M}_e$ : Element consistent mass matrix
$\mathbf{T}_1$, $\mathbf{T}_2$ : Transfer matrices
$\mathbf{T}_c$ : Point transfer matrix due to the crack
$\mathbf{T}_e^c$ : Transfer matrix of cracked element
$\mathbf{V}_i$, $\mathbf{V}_j$, $\mathbf{V}_L$, $\mathbf{V}_R$ : State vectors at positions $i$, $j$, $C_L$, $C_R$
$x_i$, $x_j$, $x_L$, $x_R$ : Translations at positions $i$, $j$, $C_L$, $C_R$
$\theta_i$, $\theta_j$, $\theta_L$, $\theta_R$ : Rrotations at positions $i$, $j$, $C_L$, $C_R$
$\omega$ : Eigenfrequency of the rotor
$\omega_{c1}$, $\omega_{c2}$, $\omega_{c3}$ : First three eigenfrequencies of cracked rotor
$\omega_{n1}$, $\omega_{n2}$, $\omega_{n3}$ : First three eigenfrequencies of uncracked rotor

## References

[1] J. Wauer, On the dynamics of cracked rotors: a literature survey, *Applied Mechanics Review*, 43 (1) (1990) 13-17.

[2] R. Gasch, A survey of the dynamic behavior of a simple rotating shaft with a transverse crack, *Journal of Sound and Vibration*, 160 (2) (1993) 313-332.

[3] A. D. Dimarogonas, Vibration of cracked structures: a state of the art review, *Engineering Fracture Mechanics*, 55 (5) (1996) 831-857.

[4] Y. P. Pu, J. Chen and J. Zou, Quasi-periodic vibration of cracked rotor on flexible bearings, *Journal of Sound and Vibration*, 215 (5) (2002) 875-890.

[5] Y. P. Pu, J. Chen and J. Zou, The research on nonlinear characteristics of a cracked rotor and reconstruction of the crack forces, *Proceedings of IMechE, Part C, Journal of Mechanical Engineering Science*, 216 (11) (2002) 1099-1108.

[6] J. Zou, J. Chen and Y. P. Pu, On the wavelet time-frequency analysis algorithm in identification of a cracked rotor, *Journal of Strain Analysis for Engineering Design*, 37 (3) (2002) 239-246.

[7] C. A. Papadopoulos and A. D. Dimarogonas, Coupled longitudinal and bending vibrations of a rotating shaft with an open crack, *Journal of Sound and Vibration*, 117, (1) (1987) 81-93.

[8] A. S. Sekhar, Vibration characteristics of a cracked rotor with two open cracks, *Journal of Sound and Vibration*, 223, (4) (1999) 497-512.

[9] H. Baruh and S. Ratan, Damage detection in flexi-

ble structures, *Journal of Sound and Vibration*, 166 (1) (1993) 21-30.

[10] S. Ratan, H. Baruh and J. Rodriguez, On-line identification and location of rotor cracks, *Journal of Sound and Vibration*, 194, (1) (1996) 67-82.

[11] M. Krawczuk and W. M. Ostachowicz, Transverse natural vibrations of a cracked beam loaded with a constant axial force, *Transactions of the ASME, Journal of Vibration and Acoustics*, 115 (4) (1993) 524-528.

[12] D. Armon, Y. B. Haim and S. Braun, Crack detection in beams by rank-ordering of eigenfrequency shifts, *Mechanical Systems and Signal Processing*, 8 (1) (1994) 81-91.

[13] Y. S. Lee and M. J. Chung, A study on crack detection using eignenfrequency test data, *Computers and Structures*, 77 (3) (2000) 327-342.

[14] R. D. Adams, P. Cawley, C. J. Pye, et al., A vibration technique for non-destructively assessing the integrity of structures, *Journal of Mechanical Engineering Science*, 20 (2) (1978) 93-100.

[15] P. Cawley and R. D. Adams, The location of defects in structures from measurements of natural frequencies, *Journal of Strain Analysis for Engineering Design*, 14 (2) (1979) 49-57.

[16] T. G. Chondros and A. D. Dimarogonas, Identification of cracks in welded joints of complex structures, *Journal of Sound and Vibration*, 69 (4) (1980) 531-538.

[17] P. F. Rizos, N. Aspragathos and A. D. Dimarogonas, Identification of crack location and magnitude in a cantilever beam from the vibration modes, *Journal of Sound and Vibration*, 138 (3) (1990) 381-388.

[18] T. Inagaki, H. Hanki and K. Shiraki, Transverse vibrations of a general cracked-rotor bearing system, *Transactions of the ASME, Journal of Mechanical Design*, 104 (2) (1982) 345-355.

[19] M. D. Rajab and A. A. Sabeeh, Vibrational characteristics of cracked shafts, *Journal of Sound and Vibration*, 147 (3) (1991) 465-473.

[20] P. Gudmundson, Eigenfrequency changes of structures due to cracks, notches or other geometrical changes, *J Mech. Phys. Solids*, 30, (5) (1982) 339-353.

[21] P. Gudmundson, The dynamic behavior of slender structures with cross-sectional cracks, *J Mech. Phys. Solids*, 31 (4) (1983) 329-345.

[22] G. Gounaris and A. D. Dimarogonas, A finite element of a cracked prismatic beam for structural analysis, *Computers and Structures*, 28 (3) (1988) 309-313.

[23] P. G. Nikolakopoulos, D. E. Katsareas, and C. A. Papadopoulos, Crack identification in frame structures, *Computers and Structures*, 64 (1) (1997) 389-406.

[24] M. W. Suh, M. B. Shim, and M. Y. Kim, Crack identification using hybrid neuro-genetic technique, *Journal of Sound and Vibration*, 238 (4) (2000) 617-635.

[25] J. L Hu and R. Y Liang, An integrated approach to detection of cracks using vibration characteristics, *Journal of the Franklin Institute*, 330 (5) (1993) 841-853.

[26] A. D. Dimarogonas, *Vibration Engineering*, St Paul, West Publishing Cooperation, (1976).

[27] G. M. Dong, J. Chen and J. Zou, Parameter identification of a rotor with an open crack, *European Journal of Mechanics A/Solids*. 23 (1) (2004) 325-333

**Guang Ming Dong** received his B.S. and M.S. degrees in Mechanical Engineering from Xi'an Jiao Tong University, China, in 1999 and 2002, respectively. He then received his Ph.D. degree in Mechanical Engineering from Shanghai Jiao Tong University, China, in 2007. Dr. Dong is currently a postdoctoral research fellow at the State Key Laboratory of Mechanical System and Vibration in Shanghai Jiao Tong University, China. Dr. Dong's research interest is on damage identification and health monitoring of structural and mechanical systems using global methods, specifically, vibration-based damage detection.

**Jin Chen** received his B.S. and M.S. degrees in Mechanical Engineering from Shanghai Jiao Tong University (SJTU), China, and his Ph.D. degree from Tokyo Institute of Technology, Japan. He is currently a professor and Ph.D. supervisor in Shanghai Jiao Tong University, the Director of the SJTU Library, and vice director of State Key Laboratory of Mechanical System and Vibration. Dr. Chen is also a member of the Standing Committee of the Chinese Society of Vibration Engineering, president of the Fault Diagnosis Society of China, Editor of the Journal of Mechanical System and Signal Processing, Standing Editor of the Journal of Vibration, Testing, and Diagnostics, and Chairman of the Alumni Association of Tokyo Institute of Technology in Shanghai.